Available online at www.sciencedirect.com
ScienceDirect
Dyes and Pigments 78 (2008) 179–198
DYES and PIGMENTS
www.elsevier.com/locate/dyepig

Analysis of the catalytic fading of pyridone-azo disperse dyes on polyester using the semi-empirical, molecular orbital PM5 method

Yasuyo Okada [a,*], Toshio Hihara [b], Zenzo Morita [c]

[a] School of Domestic Science, Otsuma Women's University, Sanban-cho, Chiyoda-ku, Tokyo 102-8357, Japan
[b] Technical Center, DyStar Japan Ltd., Shinkai-machi 2-65, Omuta, Fukuoka-ken 836-0017, Japan
[c] Tokyo University of Agriculture and Technology, Koganei, Tokyo 184-8588, Japan

Received 12 October 2007; received in revised form 3 December 2007; accepted 3 December 2007
Available online 8 December 2007

Abstract

The catalytic fading of combination dyeings on polyester fabric of six pyridone-azo and one quinolone-azo yellow disperse dyes imparted by C.I. Disperse Blue 165 as a result of exposure to a carbon arc in air was analyzed in terms of reactivity (k_0) towards singlet oxygen and the photosensitivity (f) of the dyes. Based on the assumption that the rate of photo-fading of single dyeings is proportional to the product of k_0 and f, the fading behavior of both single and mixture dyeings was explained. The k_0 values for the seven azo dyes could be correlated to the sum of electrophilic frontier densities determined using the PM5 method. The nitro groups in the pyridone-azo dyes decreased the reactivity of the electron density in parts of the diazo component. Disperse dyes with excellent light fastness on polyester exhibit low values of both f and k_0. The f values observed for the combination dyeings did not show simple additivity.

Keywords: Pyridone-azo dye; Catalytic fading; Photo-oxidation; Singlet oxygen; PM5; Poly(ethylene terephthalate)

1. Introduction

Catalytic fading is defined as the ''mutual negative influence on the light fastness (LF) of dyes in combination dyeing'' [1]. It involves blue 'eating' dye combinations or blue 'eating' yellow dyes, in which the addition of yellow and orange dyes results in preferential and accelerated fading of blue dyes. Catalytic fading applies to direct, vat, and reactive dyes on cellulose, as well as to disperse dyes on poly(ethylene terephthalate) (PET).

When two dyes with considerably different photosensitivities are placed on the same substrate, there should be no mutual negative influence on LF, relative to the LF obtained with the same concentrations of the individual dyes. One dye must be negative and the other positive; moreover no additivity of photosensitivity occurs. In terms of catalytic fading, it is important to consider ''the negative influence on the LF of partner dyes in combination dyeings''. However, it must also be taken into consideration that the amounts of light and oxygen that enter into the dyed substrate are limited and shared by the two dyes. When the negative effect on LF predominates in combination dyeings with opponent colors, catalytic fading occurs.

The mutual influences on fading behavior in binary combination dyeings of cellulose film have been analyzed in detail [2–4]. In principle, dyes with higher levels of photosensitivity have greater negative influences on the LF of the partner dyes, which is linked to greater susceptibilities of the dyes to fading by photo-oxidation. Dyes of all classes and all shades exert active and passive influences, although the extent of this influence varies widely with the specific dye. Substrates, such as wool, which can quench singlet oxygen can counteract the fading of dyes present on the

* Corresponding author. Tel.: +81 3 5275 5763; fax: +81 3 5275 7015.
E-mail address: yasuyo.okada@otsuma.ac.jp (Y. Okada).

0143-7208/$ - see front matter © 2007 Elsevier Ltd. All rights reserved.
doi:10.1016/j.dyepig.2007.12.001

substrate. In the case of cellulose dyeings, reactive and vat dyes with high levels of photosensitivity exhibit a close relationship between the rate of photo-reduction, which relates to perspiration–light fastness or tendering activity, and photosensitivity, which reflects the property of catalytic fading of the partner dyes [5].

On the other hand, in the case of PET dyeings, some disperse dyes, especially azo dyes, are known to exert negative influences on the LF of partner dyes in combination dyeings. Although in practice, some yellow dyes suffer lowering of LF in combination dyeings with blue dyes (yellow-eating blue dyes), we have no procedure to estimate the ease with which the yellow dyes are photo-oxidized and the photosensitivity of the blue dyes on the PET substrate. However, we have reported recently a procedure to estimate theoretically the ease with which reactive dyes are photo-oxidized as the values of electrophilic frontier densities using the semi-empirical molecular orbital (MO) PM5 method [6–9].

It has been known that dyes are normally oxidized in light due to fading by atmospheric oxygen, although in certain cases, fading is due to reduction [10]. In general, disperse dyeings of PET gives the highest level of LF, whereas disperse dyeings of nylon gives the lowest level of LF [11]. C.I. Disperse Blue 165 is a typical azo dye, with an LF 6 rating on PET and an LF 1 rating on nylon. The irradiation of Blue 165 on a nylon fabric results in a considerable color change, which may be attributed to the photo-reduction of nitro groups, but gives no color change on PET fabric. Assuming that only photo-oxidation occurs during light fading, the photo-fading of disperse dyes on a PET fabric was analyzed. The existence of catalytic fading of mixture dyes on PET fabrics may confirm the role of photo-oxidation in fading [12–15].

In the present study, Blue 165 (a typical partner-eating blue dye) was selected as a yellow-eating blue dye, while pyridone-azo dyes were used as the yellow dyes, which were applied at almost the same absorbance as blue dyes at their λ_{max} values. Blue 56 was also used as a typical non-eating blue dye for comparative purposes. The photo-fading behaviors of green PET fabric dyed with these dyes were analyzed, to elucidate the catalytic fading in terms of the same parameters as those examined for reactive dyes used in cellulose dyeings [6–9]. The rates of reaction ($k_{0,i}$) of the dyes towards $^1O_2$ were estimated by the PM5 method. With the assumption that the rates of fading on PET are proportional to the product of $k_{0,i}$ and the photosensitivities of the dyes, the fading behaviors of the single and combination dyeings of PET were analyzed.

2. Experimental

2.1. Dyes

Seven yellow disperse dyes (six pyridone-azo dyes and one quinolone-azo dye), Blue 165 (a yellow-eating blue dye), and Blue 56 (a non-eating blue dye) were used. The chemical structures of the azo (AT) and hydrazone tautomers (HT) of these dyes, which were detected predominantly on the PET substrate (cf. Section 3.1.1), are given below, together with the C.I. Generic Names, the C.I. Constitution Numbers, where available, (abbreviations in parentheses) and the tautomer with the largest stability on PET. The CAS registry number is given for Blue 56, since a C.I. Constitution Number is not available for the dye. The LFs of the dyes used are listed in Table 1.

2.1.1. Pyridone-azo dyes

(1) C.I. Disperse Yellow 211, C.I. 12755, (Yellow 211), HT

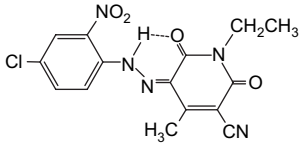

Table 1
Photochemical properties of pyridone-azo and quinolone-azo disperse dyes (*N*/2) in single dyeings of PET substrates, and analyses of their fading properties in combination dyeings with C.I. Disperse Blue 165 (*N*/3) upon exposure to a carbon arc

Dye	LF Ratings	λ_{max} on PET (nm)	Order for the slope of fading			Relative values				
			Single[a] Tab. 5	Mix. with Blue 165		$k_{0,i}/k_{0,B165}$[b]		f_i/f_{Nitro}[b]	f_i/f_{B165}	$k_{0,i}\,f_i$
				Direct	Y-51 filter	Obs.	By MO			
				Tab. 5	Tab. 5	Tab. 6				
NitrophenoxyCO	6<	449	2	1	–	2.8	4.8	1.0	0.4	4.8
Yellow 211	6<	451	3	1	–	2.3	4.0	1.4	0.5	5.6
Yellow 114	6	433	4	3	2	7.1	6.2	1.3	0.4	7.9
MeO2EtOCO	6-	447	5	3	–	6.7	5.1	1.7	0.6	8.6
Yellow 241	5	438	6	3	1	5.1	3.3	3.0	1.0	9.9
Quinolone	4–5	437	7	6	3	8.3	7.2	2.3	0.8	17
n-OctylaminoCO	4+	421	8	7	4	9.6	1.6	29.0	9.9	39
Blue 165	6<	629	1	–	–	–	1.0	2.9	1.00	2.9

[a] ΔE^*_{ab} on exposure had the same order of increase by the exposure (Table 8).
[b] cf. Table 5.

(2) C.I. Disperse Yellow 241, C.I. 128450, (Yellow 241), HT

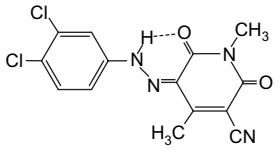

(3) C.I. Disperse Yellow 114, C.I. 128455 (Yellow 114), HT

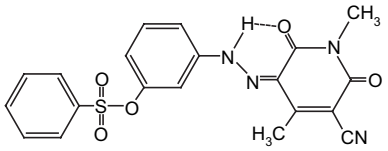

(4) A yellow *n*-octylaminocarbonyl dye, (*n*-OctylaminoCO), HT

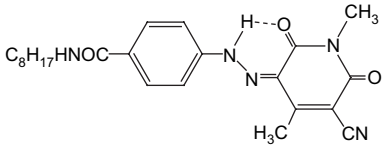

(5) A yellow methoxyethoxyethoxycarbonyl dye, (MeO2EtOCO), HT

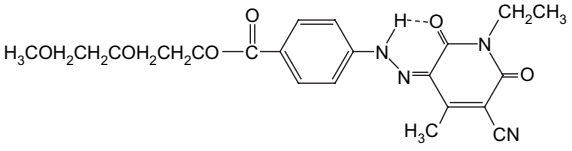

(6) A nitro-*n*-pentanoxycarbonyl dye, (NitropentanoxyCO), HT

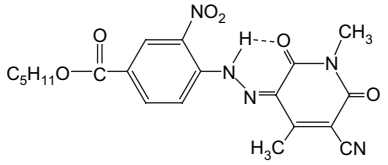

(7) A quinolone-azo dye, (Quinolone), HTs

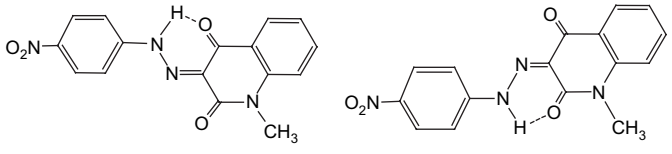

A-type (HT-A) B-type (HT-B)

2.1.2. Yellow-eating blue dye

(1) C.I. Disperse Blue 165, C.I. 11077, (Blue 165), AT

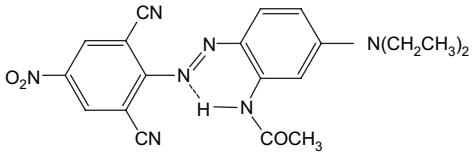

2.1.3. Yellow-non-eating blue dye

(1) C.I. Disperse Blue 56, CAS Registry Number 31810-89-6, (Blue 56)

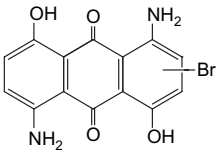

2.2. Materials, dyeing method and method of exposure

The PET fabric used was double pique grade F1142 (dtex/filament: 84/36; weight: 240 g m^{-2}; Toray Industries Inc.). The dyeing was carried out at 135 °C for 30 min in acetic acid/sodium acetate buffer (pH 4.5) at a liquor ratio of 1:20 with C.I. Disperse Blue 165 (*N*/3 depth) or Blue 56 (*N*/3 depth) and/or yellow dyes (*N*/2 depth), respectively, in both the single and combination formulations. After dyeing, reduction clearing was performed at 80 °C for 15 min under the following conditions: NaOH (2.0 g dm^{-3}), $Na_2S_2O_4$ (2.0 g dm^{-3}), and the nonionic surfactant Sera Wash M-SF (DyStar Co., Ltd.) (1.0 g dm^{-3}). Rinsing and drying were carried out after the reduction clearing. The concentrations of dyes on the PET fabric were determined by measuring the reflectance spectra with a V-550 UV–vis spectrophotometer that was equipped with an integrating sphere (Jasco Co. Ltd). The CIE chromaticity parameters of the original dyed PET fabrics are listed in Table 8. The dyed fabrics were exposed to a carbon arc using a fadeometer (Suga Test Instruments Co., Ltd).

2.3. Kubelka–Munk parameter

In order to perform quantitative analysis, the Kubelka–Munk parameter (*K*/*S*) was calculated by:

$$K/S = \frac{(1-R)^2}{2R} = \alpha C, \tag{1}$$

where R is the percentage reflectance divided by 100, C is the concentration of dyes on PET, and α is the calibration factor or absorption coefficient, which varies with the wavelength and dye used [16].

2.4. Semi-empirical molecular orbital calculation

All the MO calculations were carried out using CAChe MOPAC 2002 (Windows edition, version 6.1.12.33) (Fujitsu Ltd.) [17]. For the ATs and HTs of the eight dyes in the gas phase and water, structure optimization was performed to obtain the molecular parameters, which included the standard heats of formation in the gas and water phases ($\Delta_f H^o$(gas) and $\Delta_f H^o(H_2O)$ (kcal mol^{-1}), respectively), the energies of the HOMO and the LUMO (E_{HOMO} and E_{LUMO}, respectively), the electron densities in the HOMO (d_{HOMO}), the electrophilic frontier densities ($f_r^{(E)}$) and the dipole moment in the gas phase

(μ), using the PM5 method. The COSMO method was used to calculate the corresponding parameters in water. The $\Delta_f H^o$(gas) values were also estimated for the reaction intermediates of the corresponding tautomers with transition-state geometry (TSG). Structure optimization was carried out to calculate the $\Delta_f H^o$(gas) values for the reaction intermediates and products at the PM5 geometry.

3. Results and discussion

3.1. Estimation of the reactivity towards $^1O_2$ using the PM5 method

3.1.1. Azo–hydrazone tautomerism (AHT) of disperse azo dyes

As in the case of reactive azo dyes [6–9,18,19], AHT was determined by calculating the $\Delta_f H^o$(gas) and $\Delta_f H^o(H_2O)$ values in the gas and water phases, respectively, for pyridone- and quinolone-azo dyes using the PM5 method. The corresponding values calculated for the azo (AT) and hydrazone tautomers (HT) of the yellow dyes are listed in Table 2, together with the dipole moments, μ (debye), and the E_{HOMO} and E_{LUMO} values. The values for $\Delta_f H^o$(gas) and $\Delta_f H^o(H_2O)$ of the HTs for the yellow dyes were lower than those of the ATs, which indicates that all the dyes exist as HTs in the gas and water phases. This leads to the conclusion that all the dyes exist as HTs on the PET substrate [6–9], with the exception of quinolone (cf. Section 3.1.2.3).

The d_{HOMO} values at the main atomic positions of the HT for pyridone- and quinolone-azo dyes with optimized geometry are listed in Table 3, with the positions numbered below the table. The numbering system is different from that used for the chemical nomenclature. The electronic distributions in the HOMO resemble each other in terms of the positions of the molecules.

3.1.2. Reactivities of pyridone-azo dyes

The $^1O_2$ adds to the double bonds in aromatic molecules via the ene reaction and the [2 + 2] and [4 + 2] cycloadditions (cf. Section 3.1.2.1 for [4 + 2] cycloaddition). Hereafter, the term addition is used to refer to cycloaddition. These reactions sometimes compete with each other [20]. The $\Delta_f H^o$(gas) values of the reaction intermediates with TSG and with optimized geometry, as assessed by the PM5 method, as well as of the reaction products are listed in Table 4. For the seven yellow dyes examined, we found only small differences in the $\Delta_f H^o$(gas) values for the intermediates of the reaction with $^1O_2$ with TSG using the PM5 method among the potential reaction modes at the possible reaction sites, as in the cases of reactive dyes [6–9]. However, we found considerable differences in the $\Delta_f H^o$(gas) values for the reaction products, which allowed comparisons of the order of reactivities for the potential reaction modes.

According to the frontier orbital theory [21–24], the frontier electron density ($f_r^{(E)}$) for each electrophilic reaction type is the weighted sum of the squares of the coefficients of the LCAO MO. Fukui's original expression can be written as follows:

$$f_r^{(E)} = \frac{\sum_{j=1}^{N} \nu_j \left(C_r^j\right)^2 \exp\left\{-\lambda\left(E_{HOMO} - E_j\right)\right\}}{\sum_{j=1}^{N} \nu_j \exp\left\{-\lambda\left(E_{HOMO} - E_j\right)\right\}}, \tag{2}$$

where N is the total number of orbitals, ν_j is the number of electrons in the jth orbital and is usually 0, 1, or 2, C_r^j is the coefficient of the jth LCAO MO at the rth atomic position, E_j is the energy of jth orbital, and λ is a scale factor that is usually set to 3.0 in these calculations [17]. In this equation, besides the electrons in the HOMO, the contributions of electrons at the corresponding atomic sites in the MOs below the HOMO are taken into consideration, but no effects of the LUMO energy for partner reactant molecules on the electrophilic reaction are taken.

The electrophilic reactivity of the double bonds towards $^1O_2$ is described by the sum $S_{m,n}^{(E)}$, of the $f_r^{(E)}$ defined by Eq. (3) at the two adjacent atomic positions, as follows [6–9]:

$$S_{m,n}^{(E)} = \sum_{m,n} \left\{f_m^{(E)} + f_n^{(E)}\right\}, \tag{3}$$

where m and n denote the atomic positions of the corresponding double bonds. When there is an overlap, the overlap position is counted only once, and double bonds with larger values of ($f_m^{(E)} + f_n^{(E)}$) are taken into consideration one by one. The [4 + 2] addition is treated as a reaction towards a double bond.

Taking the chemical structures and the fading behaviors of the single and mixture dyeings into consideration, the seven yellow dyes used were classified into three groups: (1) C.I. Disperse Yellow 211 and NitropentanoxyCO; (2) Yellow 241, Yellow 114, and MeO2EtOCO; and (3) *n*-OctylaminoCO and Quinolone (cf. Section 3.3.2).

3.1.2.1. C.I. Disperse Yellow 211 and NitropentanoxyCO. The potential double bonds to which $^1O_2$ can add via ene reaction and/or [2 + 2] addition for Yellow 211 and NitropentanoxyCO are C1=N7, C5=C6, C9=C10, C11=C12, C9=C14, C12=C13, and C13=C14. On the other hand, Matsumoto et al. [25] have reported recently on the reversible [4 + 2] addition of $^1O_2$ to *N*-substituted 2-pyridones as a versatile chemical source of $^1O_2$. The degree of the contribution of [4 + 2] addition was analyzed by the same method, in which [4 + 2] addition of $^1O_2$ to C1 and C4 was expressed as [4 + 2] addition (C1=C4), irrespective of the nonexistence of double bond. Hereinafter, the same description is used for the other types of bonding.

3.1.2.1.1. C.I. Disperse Yellow 211. The order of reactivities derived from the $\Delta_f H^o$(gas) values for the reaction products (Table 4) is as follows:

$$\begin{aligned}&\text{ene}\,(\text{C10=C9;H(N8)}) > \text{ene}\,(\text{C14=C9;H(N8)}) \approx \text{ene}\,(\text{C1=N7;H(N8)}) \gg [4+2]\,\text{addition(C1=C4)}\\ &> [2+2]\,\text{addition(C5=C6)} \gg [2+2]\,\text{addition(C10=C9)} \approx [2+2]\,\text{addition(C14=C9)}\\ &\approx [2+2]\,\text{addition(C13=C14)} > [2+2]\,\text{addition(C11=C12)} \gg [2+2]\,\text{addition(C1=N7)}.\end{aligned} \tag{4}$$

Table 2
The $\Delta_f H^o$(gas) and $\Delta_f H^o(H_2O)$ (kcal mol^{-1}) values in the gas and aqueous phase, respectively, dipole moment, μ (debye), E_{HOMO} and E_{LUMO} for the A and HTs of yellow azo dyes in the gas phase, and $f_r^{(E)}$ for the most probable tautomer, as estimated by the semi-empirical MO PM5 method

	Yellow 211		NitropentanoxyCO		Quinolone				Blue 165		Yellow 241		Yellow 114		*n*-OctylaminoCO		MeO2EtOCO	
M.W.	361.744		427.416		324.295				405.415		337.165		424.430		423.514		428.444	
	AT	HT	AT	HT	AT	HT-A	AT-B	HT-B	AT	HT	AT	HT	AT	HT	AT	HT	AT	HT
$\Delta_f H^o$(gas)	19.482	14.588	−71.477	−77.641	21.209	15.096	17.556	15.005	107.839	122.951	22.057	16.049	−55.961	−63.007	−46.307	−55.539	−125.629	−144.411
μ	6.216	9.080	6.610	9.014	10.502	9.718	8.964	9.329	6.939	7.399	5.959	7.276	7.768	8.664	5.871	7.080	5.414	7.208
E_{HOMO}	−9.372	−9.976	−9.464	−9.992	−9.236	−9.377	−9.407	−9.325	−8.693	−9.098	−9.163	−9.478	−9.057	−9.307	−9.146	−9.435	−9.179	−9.501
E_{LUMO}	−2.217	−2.224	−2.459	−2.434	−2.089	−1.930	−1.754	−1.982	−2.327	−2.380	−1.878	−2.097	−1.779	−1.986	−1.923	−2.097	−2.019	−2.139
$\Delta_f H^o(H_2O)$	−0.058	−4.931	−93.877	−101.953	0.575	−5.889	−4.494	−6.536	85.962	101.178	6.834	−1.631	−84.717	−93.521	−70.732	−83.031	−149.845	−166.475
$f_r^{(E)}$(position) for	HT		HT		HT		HT		AT		HT		HT		HT		HT	
the most	0.267 (C1)		0.310 (C1)		0.051 (C7)		0.050 (C7)		0.208 (C3)		0.072(C14)		0.139(C14)		0.083(C14)		0.099(C14)	
probable	0.101 (N7)		0.073 (N7)		0.181 (C8)		0.181 (C8)		0.096 (C4)		0.134 (C9)		0.124 (C9)		0.104 (C9)		0.098 (C9)	
tautomer	0.288 (C5)		0.264 (C5)		0.123(C10)		0.124(C10)		0.228(C5)		0.107(C10)		0.102(C10)		0.094(C10)		0.096(C10)	
	0.088 (C6)		0.067 (C6)		0.107 (C4)		0.104 (C4)				0.165(C12)		0.063(C11)					
					0.105 (C3)		0.101 (C3)				0.088(C13)		0.166(C12)		0.326 (C1)		0.333 (C1)	
	0.045(C14)		0.053(C14)		0.099(C18)		0.098(C18)								0.034 (N7)		0.042 (N7)	
	0.076 (C9)		0.055 (C9)		0.074(C13)		0.067(C13)		0.015 (C6)		0.217 (C5)		0.344 (C1)					
			0.086(C10)		0.086(C14)		0.087(C14)		0.395 (C1)		0.035 (C6)		0.035 (N7)				0.219 (C5)	
					0.180 (C1)		0.199 (C1)		0.032 (C2)								0.036 (C6)	
															0.213 (C5)			
	0.038(C10)														0.030 (C6)			
	0.022(C11)		0.013(C11)								0.308 (C1)		0.213 (C5)					
	0.069(C12)		0.087(C12)		0.025 (C9)		0.024 (C9)		0.017 (N7)		0.032 (N7)		0.030 (C6)		0.024(C11)		0.028(C11)	
	0.045(C13)		0.022(C13)		0.014(N11)		0.010(N11)		0.129 (N8)						0.136(C12)		0.138(C12)	
											0.037(C11)		0.037(C13)		0.033(C13)		0.020(C13)	
$S_{m,n}^{(E)}$	0.865		0.908		1.006		1.011		0.532		0.818		0.973		0.641		0.923	

Table 3
The d_{HOMO} values for the HTs of the pyridone-azo disperse dyes, for the HTs and ATs of the quinolone-azo disperse dyes and for the ATs of Blue 165

Tautomer	Yellow 211[a]	NitropentanoxyCO[b]		Quinolone[c]				Yellow 241[d]	Yellow 114[e]	*n*-OctylaminoCO[f]	MeO2EtOCO[g]		Blue 165[h]
	HT	HT		HT-A	AT-B	HT-B		HT	HT	HT	HT		AT
C1	0.178	0.191	C1	0.099	0.007	0.110	C1	0.182	0.202	0.207	0.202	C1	0.217
C2	0.002	0.000	C2	0.001	0.001	0.001	C2	0.003	0.003	0.004	0.003	C2	0.008
N3	0.004	0.003	C3	0.036	0.091	0.035	N3	0.005	0.005	0.005	0.005	C3	0.093
C4	0.000	0.000	C4	0.046	0.113	0.043	C4	0.002	0.002	0.002	0.002	C4	0.053
C5	0.186	0.156	N5	0.171	0.274	0.170	C5	0.119	0.119	0.128	0.127	C5	0.118
C6	0.051	0.035	C6	0.004	0.016	0.003	C6	0.015	0.014	0.016	0.018	C6	0.002
N7	0.058	0.040	C7	0.029	0.039	0.027	N7	0.015	0.017	0.019	0.022	N7	0.001
N8	0.267	0.280	C8	0.093	0.187	0.089	N8	0.222	0.259	0.262	0.274	N8	0.098
C9	0.022	0.029	C9	0.003	0.015	0.002	C9	0.072	0.069	0.061	0.055	C9	0.001
C10	0.013	0.046	C10	0.071	0.112	0.069	C10	0.049	0.041	0.051	0.050	C10	0.013
C11	0.002	0.003	N11	0.007	0.002	0.005	C11	0.012	0.015	0.007	0.010	C11	0.000
C12	0.017	0.046	N12	0.160	0.008	0.164	C12	0.087	0.091	0.080	0.079	C12	0.010
C13	0.009	0.008	C13	0.035	0.001	0.032	C13	0.030	0.010	0.012	0.004	C13	0.000
C14	0.021	0.026	C14	0.040	0.001	0.043	C14	0.028	0.062	0.045	0.052	C14	0.012
N15	0.000	0.000	C15	0.004	0.000	0.003	Cl(15)	0.051	–	–	–	N15	0.000
O16	0.002	0.002	C16	0.067	0.000	0.067	Cl(16)	0.016	–	–	–	O16	0.000
O17	0.001	0.000	C17	0.001	0.000	0.001						O17	0.000
Cl(18)	0.011		C18	0.047	0.000	0.048						C18	0.000
			N19	0.000	0.000	0.000						C19	0.000
			O20	0.005	0.000	0.004						N20	0.274
			O21	0.004	0.000	0.004							
			O22	0.031	0.019	0.038							
			O23	0.014	0.071	0.011							
			C24	0.005	0.009	0.005							

[a] $R_1 = Et$, $R_2 = Cl$

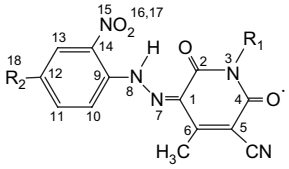

[b] $R_1 = Me$, $R_2 = n$-Pentanoxycarbonyl

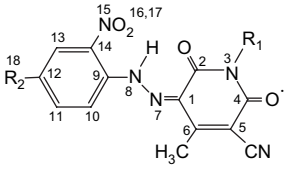

[c] As set

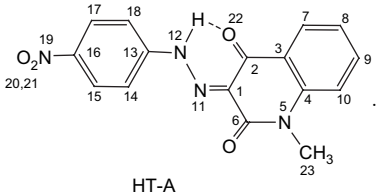

HT-A

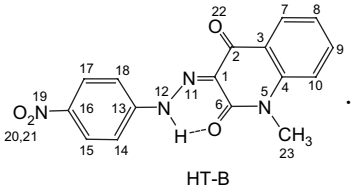

HT-B

[d] $R_1 = R_2 = Cl$

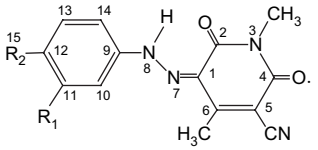

[e] R_1 = Phenylsulfonyloxy; $R_2 = H$

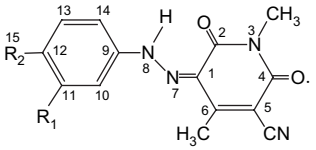

[f] $R_1 = H$; $R_2 = n$-Octylaminocarbonyl

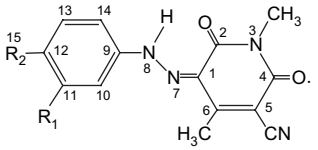

[g] As set

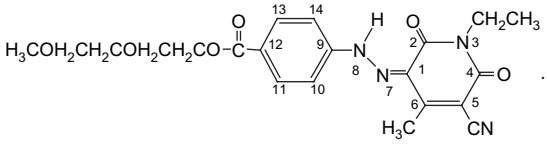

[h] As set

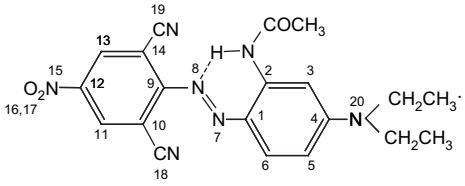

The order derived from the values of $S_{m,n}^{(E)}$ shown in Table 2 is as follows:

$$S_{5,6}^{(E)} \geq S_{1,7}^{(E)} \gg S_{9,14}^{(E)} > S_{9,10}^{(E)} = S_{12,13}^{(E)} > S_{11,12}^{(E)}. \quad (5)$$

The order for $S_{m,n}^{(E)}$ is different from the order shown in (4).

At the double bonds of C9=C10, C14=C9, and C1=N7, the ene reaction may occur more easily than [2 + 2] addition at the same site, based on the $\Delta_f H^o$(gas) values for the reaction products, although the frontier electron density does not reveal this type of priority. The [2 + 2] addition of $^1O_2$ to the double bonds of C9=C10, C11=C12, C12=C13, and C13=C14 may be excluded due to the low values of d_{HOMO} at C10 (0.013), C11 (0.002), and C13 (0.009) (Table 3). The double bond of C14=C9 contributes to the reactivity (Table 2). The $\Delta_f H^o$(gas) values for the addition products at these bonds had higher values. The [4 + 2] addition (C1=C4) may be excluded due to the low value of d_{HOMO} at C4 (0.000). Thus, only the double bonds of C1=N7, C5=C6 and C14=C9 contribute to the reactivity, as shown in Table 2.

3.1.2.1.2. NitropentanoxyCO. The order of reactivities deduced from the $\Delta_f H^o$(gas) values for the reaction products is as follows:

ene (C1=N7; H(N8)) > ene (C10=C9; H(N8)) > ene (C14=C9; H(N8)) > [2 + 2] addition(C5=C6)
> [4 + 2] addition(C1=C4) > [2 + 2] addition(C10=C9) > [2 + 2] addition(C13=C14)
≈ [2 + 2] addition(C14=C9) > [2 + 2] addition(C11=C12) ≫ [2 + 2] addition(C1=N7). (6)

Although the order of the $\Delta_f H^o$(gas) values of the reaction products for the ene reaction is different from that of Yellow 211, the double bonds of C9=C10, C11=C12, C12=C13 and C14=C9 need to be considered. Thus, the double bonds of C11=C12 and C12=C13 are excluded due to the low values of d_{HOMO} at C11 (0.003) and C13 (0.008) (Table 3). The [4 + 2] addition (C1=C4) may be excluded due to the low value of d_{HOMO} at C4 (0.000). These results are summarized in Table 2.

Although the $\Delta_f H^o$(gas) and $\Delta_f H^o(H_2O)$ values for Yellow 211 and NitropentanoxyCO differed considerably from each other, the distributions of the d_{HOMO} values listed in Table 3 and of the $f_r^{(E)}$ values listed in Table 2 are similar to each other; these two dyes possess different reactivities towards $^1O_2$ due to the different contributions to reactivity of the double bonds in the diazo component. However, since the contribution of the double bonds is not large compared to that for Yellow 211, the dipole moments are almost identical. Thus, the nitro groups in Yellow 211 decrease the electronic densities in the diazo components to the limit of reactivity, while the groups in NitropentanoxyCO have smaller effects, as mentioned above. These findings suggest a shift of electron density into the pyridone ring in the HOMO, which results in an increase of dipole moment or transition dipole moment, compared with the other pyridone-azo dyes.

3.1.2.2. Yellow 114, Yellow 241, n-OctylaminoCO, and MeO2EtOCO. The potential double bonds of C1=N7, C5=C6, C9=C10, C11=C12, C12=C13, C13=C14 and C14=C9 are classified into three groups: C1=N7 at the azo position, C5=C6 in the pyridone ring, and the remaining bonds in the diazo component (cf. Table 2), although some bonds are excluded depending on the dye structure.

The order of reactivity from the $\Delta_f H^o$(gas) values for the reaction products from the four dyes is as follows:

For Yellow 241:

ene (C1=N7; H(N8)) > ene (C10=C9; H(N8)) > ene(C14=C9; H(N8)) > [4 + 2] addition(C1=C4)
> [2 + 2] addition(C5=C6) > [2 + 2] addition(C10=C9) ≈ [2 + 2] addition(C11=C12)
≈ [2 + 2] addition(C14=C9) > [2 + 2] addition(C13=C14) ≫ [2 + 2] addition(C1=N7). (7)

For Yellow 114:

ene (C1=N7; H(N8)) > ene (C10=C9; H(N8)) > ene (C14=C9; H(N8)) > [4 + 2] addition(C1=C4)
> [2 + 2] addition(C5=C6) > [2 + 2] addition(C11=C12) > [2 + 2] addition(C10=C9)
≈ [2 + 2] addition(C14=C9) > [2 + 2] addition(C13=C14) ≫ [2 + 2] addition(C1=N7). (8)

For *n*-OctylaminoCO:

$$\begin{aligned}&\text{ene}\,(\text{C1}{=}\text{N7};\text{H(N8)}) > \text{ene}\,(\text{C10}{=}\text{C9};\text{H(N8)}) \approx \text{ene}\,(\text{C14}{=}\text{C9};\text{H(N8)}) > [4+2]\,\text{addition(C1}{=}\text{C4)}\\ &> [2+2]\,\text{addition(C5}{=}\text{C6)} > [2+2]\,\text{addition(C10}{=}\text{C9)} \approx [2+2]\,\text{addition(C14}{=}\text{C9)}\\ &> [2+2]\,\text{addition(C13}{=}\text{C14)} > [2+2]\,\text{addition(C11}{=}\text{C12)} \gg [2+2]\,\text{addition(C1}{=}\text{N7)}.\end{aligned} \tag{9}$$

For MeO2EtOCO:

$$\begin{aligned}&\text{ene}\,(\text{C1}{=}\text{N7};\text{H(N8)}) > \text{ene}\,(\text{C10}{=}\text{C9};\text{H(N8)}) \approx \text{ene}\,(\text{C14}{=}\text{C9};\text{H(N8)}) > [2+2]\,\text{addition(C5}{=}\text{C6)}\\ &> [4+2]\,\text{addition(C1}{=}\text{C4)} > [2+2]\,\text{addition(C10}{=}\text{C9)} > [2+2]\,\text{addition(C13}{=}\text{C14)}\\ &\approx [2+2]\,\text{addition(C14}{=}\text{C9)} > [2+2]\,\text{addition(C11}{=}\text{C12)} \gg [2+2]\,\text{addition(C1}{=}\text{N7)}.\end{aligned} \tag{10}$$

As shown in Tables 2 and 3, these four dyes possess similar distributions of d_{HOMO} and $f_{\mathrm{r}}^{(\mathrm{E})}$ but display small differences in the values for the atomic positions, which results in almost identical reactivities among the groups, with the exception of the *n*-OctylaminoCO group. Thus, the four dyes possess potential double bonds with reactivity towards $^1O_2$ in the diazo component, whereas the reactivities at C11 and/or C13 are excluded due to the low values of d_{HOMO}, depending on the dye. When both of these sites are excluded, C12, which is located between these bonds, is also excluded for *n*-OctylaminoCO and MeO2EtOCO. Although the double bonds of C1=N7 and C5=C6 are mentioned as the second and/or third large potential bonds with high reactivities, it is not clear that they contribute to the reactivities of these dyes because of the extremely biased distribution of electrons in the double bonds as well as the low values of d_{HOMO} at C6 and N7, although the values of $S_{m,n}^{(\mathrm{E})}$ for C1=N7 and C5=C6 are very large, if included. In the case of *n*-OctylaminoCO, both the double bonds are excluded, which results in a low value for $S_{m,n}^{(\mathrm{E})}$ and consequently, a high value for f_i (cf. Sections 3.3.2.2 and 3.3.4). This finding is consistent with the fading behavior. Unfortunately, it is difficult to decide on criteria that reflect the effectiveness of bond reactivity. The present experimental results for the three dyes gave some differences in photo-fading. The present MO method does not indicate directly the photosensitivity. The differences among the three dyes that may be attributable to reactivities could not be expressed accurately by the PM5 method as potential double bonds with significant differences. Unfortunately, no experiments have been conducted to elucidate these differences in reactivities of C1=N7 and C5=C6 among the three dyes, with the exception of *n*-OctylaminoCO.

From the fading behaviors of these three dyes in the combination dyeings, and assuming that some double bonds with low values of d_{HOMO} are excluded, the $S_{m,n}^{(\mathrm{E})}$ values for the three dyes were calculated (Table 2). For each column in which the $f_{\mathrm{r}}^{(\mathrm{E})}$ values are listed for each dye, the values below a vacant row (inserted for the classification) are included, while the values below three vacant rows are excluded.

A modification of the MO calculation: Reliable data for the criteria used in the MO calculation for *n*-OctylaminoCO are lacking. If the criteria are changed to include the contribution of the double bond: C5=C6 for *n*-OctylaminoCO, ($S_{m,n}^{(\mathrm{E})}$ becomes 0.884. As the result, $k_{0,i} = 3.67$); C5=C6 for Yellow 241, ($S_{m,n}^{(\mathrm{E})} = 1.158$, $k_{0,i} = 11.5$); and C1=N7 for Yellow 114 ($S_{m,n}^{(\mathrm{E})} = 1.216$, $k_{0,i} = 14.6$), the relative values of $k_{0,i}/k_{0,\mathrm{B165}}$ and f_i/f_{Nitro} are modified. Thus, the f value for *n*-OctylaminoCO is reduced to a third of its former value, while the $k_{0,i}$ values for Yellow 241 and Yellow 114 remain high. There are no criteria available to select a reasonable cutoff for these experiments, even if the MO calculation contains specific errors for any one of these dyes.

3.1.2.3. Quinolone. This dye carries out two types of AHT and the four types of tautomers should co-exist depending upon the Gibbs free energies [18,19]. As evidenced by the $\Delta_{\mathrm{f}}H^{\mathrm{o}}$(gas) and $\Delta_{\mathrm{f}}H^{\mathrm{o}}(\mathrm{H_2O})$ values (Table 2), the dye exists energetically as two types of HTs and a B-type of AT in the gas phase. The chemical structures of the two types of HT-A and HT-B are illustrated in Section 2.1.1.

Since the population ratios of tautomers with higher stability change when the dye is transferred into water, the picture of AHT may be complex in the PET substrate. The HT-B may exist as the predominant tautomer in PET as well as in the gas phase and water phase, although the AT-B may exist as a very small population in PET. Small differences in the distributions of d_{HOMO} between the two types of HTs were noted (Table 3). The reactivity of the HT-B is noteworthy, although MO calculations were also carried out for the HT-A (Tables 2–4), the results of which show that no comparison is required between the two types.

The double bonds to which $^1O_2$ can add are C1=N11, C3=C4, C4=C10, (C9=C10), C7=C8, C13=C14, (C13=C18), and N12=C13, and three types of [4 + 2] addition are detected. The double bonds in parentheses are

Table 4
The $\Delta_f H^o$(gas) (kcal mol^{-1}) values of the intermediate and end products in the ene and [2 + 2] addition reactions at the double bonds of C1═N7, C14═C9, C10═C9, C5═C6, C11═C12, etc. for the HTs of pyridine- and quinolone-azo dyes with singlet oxygen

Dye	Molecular weight	$\Delta_f H^o$(gas) of intermediate at TSG	$\Delta_f H^o$(gas) of intermediate	$\Delta_f H^o$(gas) of hydroperoxide	$\Delta_f H^o$(gas) of intermediate at TSG	$\Delta_f H^o$(gas) of intermediate	$\Delta_f H^o$(gas) of addition product
Mode (position)		Ene (C1═N7; H(N8))			[2 + 2] Addition (C1═N7)		
Yellow 211	393.743	38.972	39.012	1.605	38.979	38.985	34.481
NitropentanoxyCO	459.415	−53.683	−53.499	−95.210	−53.683	−53.561	−56.313
Yellow 241	369.163	39.805	39.873	−4.216	38.030	38.052	36.658
Yellow 114	456.429	−40.503	−40.502	−81.063	−38.208	−38.155	−42.922
n-OctylaminoCO	455.513	−31.712	−31.707	−74.121	−31.746	−31.742	−35.820
MeO2EtOCO	460.443	−121.162	−121.155	−163.607	−119.484	−119.479	−124.363
Mode (position)		Ene (C10═C9; H(N8))			[2 + 2] Addition (C10═C9)		
Yellow 211	393.743	39.010	39.170	−1.377	39.016	39.139	20.477
NitropentanoxyCO	459.415	−53.656	−53.647	−93.149	−53.657	−53.654	−74.294
Yellow 241	369.163	39.830	39.890	−0.221	39.730	39.764	18.814
Yellow 114	456.429	−38.533	−38.530	−79.352	−41.379	−41.371	−59.926
n-OctylaminoCO	455.513	−31.779	−31.744	−67.503	−31.771	−31.762	−52.701
MeO2EtOCO	460.443	−121.387	−121.349	−156.115	−121.479	−121.315	−141.208
Mode (position)		Ene (C14═C9; H(N8))			[2 + 2] Addition (C14═C9)		
Yellow 211	393.743	39.030	39.042	1.568	39.049	39.106	21.100
NitropentanoxyCO	459.415	−53.702	−53.647	−87.970	−54.808	−54.801	−71.535
Yellow 241	369.163	39.549	39.549	4.039	40.065	40.107	19.413
Yellow 114	456.429	−38.826	−38.825	−74.707	−40.702	−40.692	−59.892
Mode (position)		Ene (C1═N11; H(N12))			[2 + 2] Addition (C1═N11)		
Quinolone A	356.294	40.342	40.399	−2.972	40.364	40.364	37.145
Quinolone B	356.294	38.933	38.937	−2.800	49.956	49.964	42.449
Mode (position)		Ene (C14═C13; H(N12))			[2 + 2] Addition (C14═C13)		
Quinolone A	356.294	40.421	40.450	6.739	40.419	40.463	22.978
Quinolone B	356.294	40.400	40.412	4.807	50.500	50.500	22.978

Dye	Molecular weight	$\Delta_f H^o$(gas) of intermediate at TSG	$\Delta_f H^o$(gas) of intermediate	$\Delta_f H^o$(gas) of addition product	$\Delta_f H^o$(gas) of intermediate at TSG	$\Delta_f H^o$(gas) of intermediate	$\Delta_f H^o$(gas) of addition product
Mode (position)		[2 + 2] Addition (C5═C6)			[2 + 2] Addition (C11═C12)		
Yellow 211	393.743	39.073	39.083	11.544	39.078	39.100	22.363
NitropentanoxyCO	459.415	−53.690	−53.628	−83.424	−53.884	−53.859	−67.630
Yellow 241	369.163	40.154	40.165	10.821	39.910	39.924	19.046
Yellow 114	456.429	−38.545	−38.545	−67.744	−40.330	−40.314	−61.657
n-OctylaminoCO	455.513	−31.653	−31.651	−60.093	−31.832	−31.831	−48.650
MeO2EtOCO	460.443	−122.792	−122.765	−149.206	−114.368	−114.368	−138.245
Mode (position)		[2 + 2] Addition (C13═C14)			[4 + 2] Addition (C1═C4)		
Yellow 211	393.743	39.016	39.045	21.360	39.061	39.076	9.865
NitropentanoxyCO	459.415	−54.827	−54.789	−72.012	−52.379	−52.369	−78.957
Yellow 241	369.163	39.844	39.844	20.712	38.315	38.392	8.180
Yellow 114	456.429	−25.415	−25.366	−57.197	−30.975	−30.968	−70.103
n-OctylaminoCO	455.513	−31.801	−31.801	−51.781	−31.451	−31.451	−61.959
MeO2EtOCO	460.443	−119.031	−119.031	−140.224	−105.962	−105.960	−144.106
Mode (position)		[2 + 2] Addition (C3═C4)			[2 + 2] Addition (C7═C8)		
Quinolone A	356.294	40.084	40.085	27.180	40.379	40.380	19.641
Quinolone B	356.294	50.412	50.414	23.784	38.888	39.037	19.629
Mode (position)		[2 + 2] Addition (C9═C10)			[2 + 2] Addition (N12═C13)		
Quinolone A	356.294	40.352	40.085	20.165	–	–	–
Quinolone B	356.294	38.911	38.951	19.597	40.368	40.414	44.516
Mode (position)		[2 + 2] Addition (C10═C4)			[4 + 2] Addition (C1═C4)		
Quinolone A	356.294	40.319	40.319	20.592	40.391	40.392	19.006
Quinolone B	356.294	49.986	49.992	19.904	38.714	38.733	18.821
Mode (position)		[4 + 2] Addition (C4═C8)			[4 + 2] Addition (C7═C10)		
Quinolone A	356.294	40.469	40.472	12.697	40.475	40.480	5.853
Quinolone B	356.294	39.158	39.162	11.196	39.136	39.136	5.550

symmetric to the former bonds. The values of $\Delta_f H^o$(gas) for the reaction intermediates and the products for the corresponding reaction modes at these double bonds were calculated for two types of HTs (HT-A and HT-B) using the PM5 method, and the results are shown in Table 4. No calculation was performed for the symmetric bonds, but the corresponding reaction modes were regarded as giving the same results. The order of reactivity deduced from the $\Delta_f H^o$(gas) values of the reaction products for the HT-B is as follows:

$$\begin{aligned}&\text{ene}\,(\text{C1}{=}\text{N11};\text{H(N12)}) > \text{ene}\,(\text{C14}{=}\text{C13};\text{H(N12)}) \approx [4+2]\,\text{addition(C7}{=}\text{C10)} \gg [4+2]\,\text{addition(C4}{=}\text{C8)}\\ &> \text{ene}\,(\text{C18}{=}\text{C13};\text{H(N12)}) \approx [4+2]\,\text{addition(C1}{=}\text{C4)} \approx [2+2]\,\text{addition(C9}{=}\text{C10)} \approx [2+2]\,\text{addition(C7}{=}\text{C8)}\\ &\approx [2+2]\,\text{addition(C10}{=}\text{C4)} > [2+2]\,\text{addition(C14}{=}\text{C13)} \approx [2+2]\,\text{addition(C18}{=}\text{C13)}\\ &> [2+2]\,\text{addition(C3}{=}\text{C4)} \gg [2+2]\,\text{addition(C1}{=}\text{N11)} > [2+2]\,\text{addition(N12}{=}\text{C13)}. \end{aligned} \tag{11}$$

The results for the symmetric double bonds are regarded as having the same values for $\Delta_f H^o$(gas) as those depicted by the order in (11). Although the d_{HOMO} values at C15 and C17 are low, due to the similarities with pyridone-azo dyes, the following conclusions can be drawn:

1. The $\Delta_f H^o$(gas) values for the reaction intermediates with TSG are almost identical for all the reaction modes examined.
2. Except for the [2 + 2] addition (C1═N11) and the [2 + 2] addition (N12═C13), the $\Delta_f H^o$(gas) values for the reaction products are lower by more than 20 kcal mol^{-1} than the values for the reaction intermediates. Almost all the reaction modes are regarded as occurring, with certain exceptions.
3. Due to the low value of d_{HOMO} at N11 (0.005), ene (C1═N11; H(N12)) is excluded, despite the high stability of the reaction products.
4. The reaction intermediates with TSG and the reaction products with PM5 geometry for the HT-B have higher stabilities than the HT-A, with one exception.
5. The [4 + 2] additions (C7═C10), (C4═C8), and (C1═C4) may occur, although they may be reversible. This notion has not been confirmed, although since some of the products have high stability, they may be irreversible. We did not pursue this topic further. The atomic positions other than C1 contribute to the other reaction modes. If the C1 position is regarded as contributing to the reactivity as a [4 + 2] addition, this dye has the largest value of $k_{0,i}$ and average value of f. The contribution of C1 was taken into consideration, since this dye shows relatively high reactivity.
6. The differences in the $\Delta_f H^o$(gas) values for the reaction intermediates and the products for various modes between two types of HTs are reduced in line with the modes as well as the reaction courses. Tautomerism between the two types of HTs or two AHTs occurs in the reaction with $^1O_2$.

The results are summarized in Table 2. Quinolone shows a high $f_r^{(E)}$ value, which eventually exceeds the corresponding values for the pyridone-azo dyes without nitro groups. However, if the [4 + 2] addition is reversible, the practical value may contain some ambiguity. Moreover, since the predominant tautomers of this dye in PET could not be unequivocally determined by the PM5 method, the reactivity may be uncertain.

3.1.2.4. Reactivity of C.I. Reactive Blue 165. In order to elucidate the catalytic fading of the seven yellow dyes using Blue 165 as the photo-sensitizer, the blue dye was examined by the same method. The same values for the parameters calculated by the PM5 method are listed in Table 2. Blue 165 exists as an AT on the PET substrate (Table 2) and has low reactivity compared to the seven yellow dyes, although no detailed analyses were carried out. The results shown in Tables 2 and 3 indicate that the only potential double bonds are C3═C4 and C4═C5, and that the other atomic positions are excluded from the reactivity due to the alternate distribution of d_{HOMO} in the diazo component and the small d_{HOMO} and $f_r^{(E)}$ values at C2, C6 and N7.

3.1.2.5. Reactivities of yellow disperse azo dyes. Based on the results of the $f_r^{(E)}$ listed in Table 2, the order of reactivities deduced from the $S_{m,n}^{(E)}$ values is as follows:

$$\begin{aligned}&\text{Quinolone} > \text{Yellow 114} > \text{MeO2EtOCO} > \text{NitropentanoxyCO} > \text{Yellow 211} > \text{Yellow 241} > n\text{-OctylaminoCO}\\ &> (\text{Blue165}). \end{aligned} \tag{12}$$

The differences in reactivity among the four dyes of group (2), including *n*-OctylaminoCO (cf. Section 3.3), are dependent upon whether or not the double bonds of C1═N7 and/or C5═C6 participate in the reaction, although the double bonds in the diazo component are involved differently in the reactivity. The criteria of participation for double bonds are the thresholds of $f_r^{(E)}$ and d_{HOMO}.

The substituents in the diazo components of the six pyridone-azo dyes examined had little effect on the distribution d_{HOMO} (Table 3), as shown practically by the λ_{max} of the dyes on PET (Table 1). No substituents other than the nitro group in all the pyridone-azo dyes used had any effect on the d_{HOMO} in the pyridone ring. Thus, yellow disperse (pyridone-azo and quinolone-azo) dyes possess a rather narrow range of properties, which results in some scattering of the experimental results. The selection of dyes with yellow and blue hues to examine catalytic fading is necessary, in order to avoid enlarging the interaction, for example, photosensitization between componential dyes, although yellow dyes show a limited relationship between properties and chemical structure.

3.1.2.6. Relationship between $S_{m,n}^{(E)}$ and ln k_0. In order to demonstrate the results of frontier orbital analysis using the PM5 method, the relative values of $k_{0,i}$ for eight dyes were calculated assuming a linear relationship between $S_{m,n}^{(E)}$ (Table 2) and ln $k_{0,i}$, as in the cases of reactive dyes [6–9] (Fig. 1). The results are listed as the relative values of $k_{0,i}/k_{0,B165}$, with the value of Blue 165 set at 1.0 as the reference, in Table 5. In order to plot this relationship, a hypothetical value of $k_{0,i}$ was inserted, and the corresponding values for the other dyes could be determined. Thus, the ordinate of Fig. 1 is described as an optional scale.

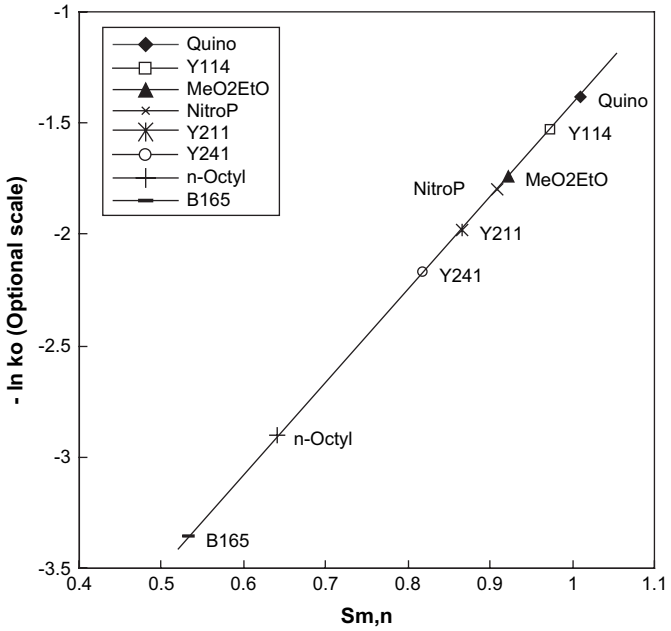

Fig. 1. Relationships between $S_{m,n}^{(E)}$ and ln k_0 for the disperse azo dyes used in this study. The name of dye is further simplified.

3.2. Photo-fading of individual yellow dyes

The fading of seven disperse azo dyes in single dyeings is illustrated in Fig. 2. Dividing the experimental slopes of fading for the single dyeings by the relative values of $k_{0,i}/k_{0,Blue165}$, the relative values for the reduced slope of fading were obtained. From the ratios to the value obtained for NitropentanoxyCO as the reference, the relative values of f_i/f_{Nitro} were calculated (Table 5). When the values of f_i/f_{Nitro} are multiplied by a factor of 1/2.90, the relative values of f_i/f_{B165} are obtained.

From the relative values, the order of f_i is as follows:

$$n\text{-OctylaminoCO} \gg \text{Yellow 241} > (\text{Blue 165}) > \text{Quinolone} > \text{MeO2EtOCO} > \text{Yellow 211} > \text{Yellow 114} > \text{NitropentanoxyCO}. \quad (13)$$

The extremely large value for *n*-OctylaminoCO stems from the low estimation of $k_{0,i}$. In fact, *n*-OctylaminoCO can be regarded as one of the strongest partner-eating dyes. Whether this estimation is reasonable or not represents a problem with the PM5 method. As expected from the considerable effect on catalytic fading of combination dyeings, Blue 165, Quinolone, and Yellow 211 possess higher f_i values (Table 5). The f_i value for Yellow 241, as estimated indirectly by the MO method and directly by its own slope of fading, was larger than that for MeO2EtOCO. However, since few significant differences were observed for the rate of fading of Blue 165 in the combination dyeings, compared with the rate in the mixture with MeO2EtOCO, Yellow 241 is not considered to be a strong sensitizer. The differences in the fading behaviors for the dyes in group (2) in the single and combination dyeings remain to be resolved (cf. Sections 3.1.2.2 and 3.4). The rates of fading for Yellow 211 in the single dyeings were almost the same as those for mixture dyeings with Blue 165, while those for the other dyes in single dyeings were always lower than those in mixture dyeings (Table 5). This finding indicates that Blue 165 accelerates or sensitizes the fading of the yellow dyes examined. These results indicate that the simple principle of introducing $k_{0,i}$ and f_i values is reasonable. As the results show, the f_i values obtained from the single dyeings were consistent with the values exhibited in the mixture dyeings.

Based on the estimated $k_{0,i}$ and f_i values, the fading behaviors of the combination dyeings are analyzed below.

3.3. Photo-fading of individual yellow dyes on PET fabrics in combination dyeings with C.I. Disperse Blue 165

3.3.1. Analysis of catalytic fading of yellow dyes by blue dyes

In order to estimate the fading of individual dyes in the combination dyeings, the Kubelka–Munk equation (1) was used by transforming the reflectances at the λ_{max} of each dye into the *K*/*S* values (cf. Section 2.3). Although little absorption of yellow dyes exists at the λ_{max} of blue dyes, as the weak absorption of blue dyes exists at the λ_{max} of yellow

Table 5
Analyses of the rates of fading of disperse azo dyes in single and mixture dyeings of PET fabric upon exposure to a carbon arc in air

Dye	Single dyeings						Mixture dyeing with Blue 165		
	Slope[a,b]	Relative values[b]					No filter[e]	Y-51 filter[e]	Ratio of slope[f]
	$-\ln\frac{(KSR)_t}{(KSR)_0}/t$	$k_{0,i}/k_{0,B165}$ by MO	Reduced slope[c]	f_i/f_{Nitro}	f_i/f_{B165}	$k_{0,i}f_i$[d]	$-\ln\frac{(KSR)_t}{(KSR)_0}/t$		
NitropentanoxyCO	0.979_1 (2)	4.76 (5)	0.206	1.00 (1)	0.35	4.76 (2)	1.06	–	–
Yellow 211	1.14_4 (3)	3.97 (4)	0.288	1.40 (3)	0.48	5.56 (3)	1.29	–	–
Yellow 114	1.61_1 (4)	6.23 (7)	0.259	1.26 (2)	0.43	7.85 (4)	3.05	0.213	14
MeO2EtOCO	1.76_5 (5)	5.05 (6)	0.350	1.70 (4)	0.59	8.59 (5)	2.74	–	–
Yellow 241	2.03_7 (6)	3.29 (3)	0.619	3.00 (7)	1.04	9.87 (6)	2.73	0.0788	35
Quinolone	3.45_0 (7)	7.24 (8)	0.477	2.32 (5)	0.80	16.8 (7)	6.33	0.647	10
n-OctylaminoCO	9.37_6 (8)	1.58 (2)	5.93	28.8 (8)	9.93	45.5 (8)	9.74	0.943	10
Blue 165	0.596_6 (1)	1.00 (1)	0.597	2.90 (6)	1.00	2.90 (1)	–	–	–

[a] $\times 10^6$ (s^{-1}), average value described as the slope by exposure for 20–40 h.
[b] Parenthesis describes the order.
[c] $\times 10^6$ (s^{-1}), divided by the relative values of $k_{0,i}/k_{0,B165}$.
[d] $k_{0,i}/k_{0,B165} \times f_i/f_{Nitro}$.
[e] $\times 10^6$ (s^{-1}), average value described as the slope by exposure for 20–60 h.
[f] Ratio of slopes for the fading between the direct exposure and the exposure through Y-51 filter.

dyes, the original *K*/*S* values of the yellow dyes, $(K/S)_{original}$, were reduced by the corresponding values overlapping the real values. Plotting the logarithms of the relative reduced values of *K*/*S* after exposure, $(KSR)_t/(KSR)_0$, against the time of exposure, the rates of fading for seven yellow dyes could be estimated from the slopes of the plots, as illustrated in Fig. 3(a) and listed in Table 5.

The photo-oxidative fading of the seven yellow dyes sensitized by Blue 165 may be explained as being similar to that of reactive dyes on cellulose [2–4]. The photo-fading of dyes occurs at the surface of the fabric, from which light enters into the PET substrate followed by diffuse reflection, and oxygen penetrates from the surface of each filament. Evans [11] has explained this as the photochemical layer effect or the filter effect, which results from the absorption of incident radiation by the dye molecule at or near the fiber surface nearest the source of radiation. Thus, dye molecules deeper in the substrate are exposed to lower intensity radiation and fade less rapidly. Since absorbance >0.05 can cause the filter effect [26], one must take this effect into consideration for almost all dyeings.

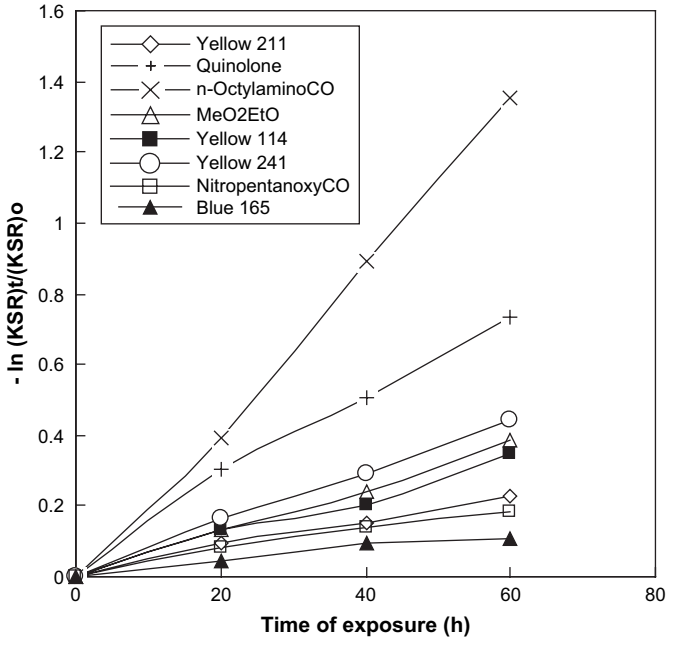

Fig. 2. Rates of fading for disperse azo dyes in single dyeings of PET upon exposure to a carbon arc in air.

On the other hand, if catalytic fading is attributed to the action of $^1O_2$, the generation of which is sensitized by effective $^1O_2$ sensitizers to accelerate the fading of the partner dye and self-sensitized oxidative fading in the single dyeings [12–14], oxygen should be supplied from the surface of the fiber, which is another surface-preferential phenomenon, since the solubility is not high enough (5.1×10^{-4} mol kg^{-1} at 25 °C). From the solubility constant of Henry's law [27], the solubility of O_2 in oriented PET in air was estimated. Although the concentrations of dyes in PET are of the order of 10^{-3} mol kg^{-1}, the consumption of oxygen by oxidative fading should be supplemented by adsorption on and the diffusion from the surface. The environment of photosensitized fading may be sufficiently prepared.

It is assumed as the first approximation that the reaction of the dye with $^1O_2$ in the PET substrate may be treated as a homogeneous system. As the result of continuous irradiation, if a sufficient amount of oxygen exists in the substrate and is supplied from the environment, steady-state generation of $^1O_2$ by the sensitization of the *i*th dye in the single dyeings may be assumed as follows:

$$[^1O_2] = [^3O_2]f_i, \tag{14}$$

where the square brackets denote concentration (mol kg^{-1}). Since we have no reference sensitizer, such as Rose Bengal or copper phthalocyanine, we selected the relative values of $k_{0,i}$ and f_i for Blue 165 as the reference, and advanced the

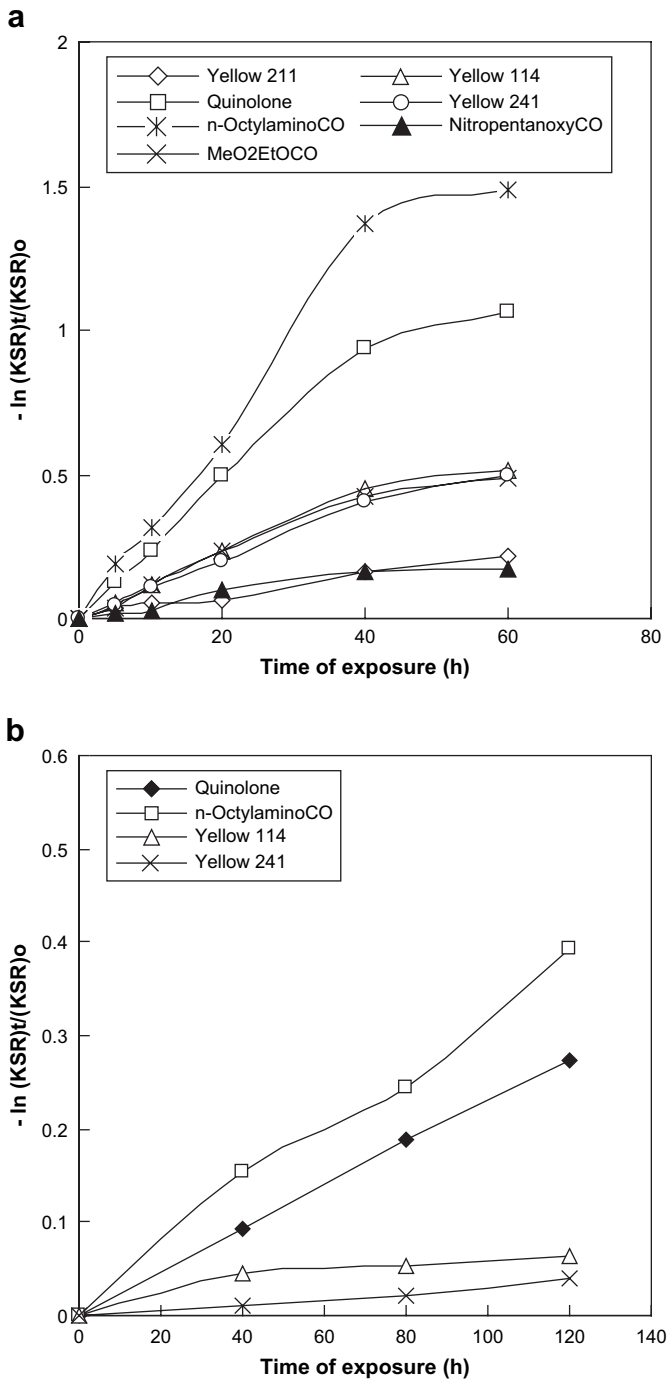

Fig. 3. Rates of fading for yellow disperse azo dyes on PET fabrics in the combination dyeings with C.I. Disperse Blue 165 upon exposure to a carbon arc in air. (a) Direct exposure and (b) exposure through a Y-51 filter.

discussion.The equation of the second-order reaction between the dye and $^1O_2$ is described as follows:

$$-\frac{d[D_i]}{dt} = k_{0,i}[^1O_2][D_i], \tag{15}$$

where t is the time of reaction and i describes the ith yellow or blue dye. Since in the initial period of irradiation, the reaction of the dye with $^1O_2$ may be regarded as being of pseudo-first-order; i.e., $[^1O_2]$ is kept constant, Eq. (15) becomes:

$$\ln\frac{[D_{t,i}]}{[D_{0,i}]} = -k_{0,i}[^1O_2]t, \tag{16}$$

where $[D_{0,i}]$ and $[D_{t,i}]$ are the initial concentration and the concentration at the time of exposure t for i-dye, respectively. If the fading of Blue 165 at the beginning is regarded as the reference, Eq. (16) becomes:

$$\frac{\ln\frac{[D_{t,i}]}{[D_{0,i}]}}{\ln\frac{[D_{t,B165}]}{[D_{0,B165}]}} = -\left(\frac{k_{0,i}}{k_{0,B165}}\right)\left(\frac{f_i}{f_{B165}}\right), \tag{17}$$

where $[D_{0,B165}]$ and $[D_{t,B165}]$ are the initial concentration and the concentration at the time of exposure t for Blue 165, respectively. Here, $k_{0,B165}$ and f_{B165} denote the $k_{0,i}$ and f_i values for Blue 165, respectively.

3.3.2. Catalytic fading of yellow dyes by blue dye

From the values of the slopes illustrated in Fig. 3(a), the classification into three groups is reasonable (cf. Section 3.1.2). The theoretical estimations that the reactivity towards $^1O_2$ for Quinolone is greater than that for dyes of group (2) and that the reactivities for these three dyes are greater than those for the dyes in group (1) were confirmed to be reasonable by the experimental results.

3.3.2.1. Dyes of groups (1) and (2). The relationships between the rates of fading against time, as illustrated for the yellow dyes in Fig. 3 (a), are analyzed below.

Group (1): Although Yellow 211 and NitropentanoxyCO possess considerably different $k_{0,i}$ values, as estimated from MO theory, they exhibited almost identical rates of fading. This suggests that following the exposure of the combination dyeings to Blue 165, the analysis leading to Eq. (17) holds strictly and the f_i values of the componential dyes have profound effects on the ratios of the rates of fading, estimated as the $k_{0,i}/k_{0,B165}$ values in the heterogeneous disperse dye-PET system.

Group (2): The Yellow 241, Yellow 114 and MeO2EtOCO dyes showed the same slopes of fading in the combination dyeings (cf. Section 3.2). As mentioned above, if the assumption leading to Eq. (17) holds strictly, the MO theory is insufficient. We should discuss whether or not the f_i values are reasonable to explain the fading behaviors.

3.3.2.2. Exceptional fading of Quinolone and n-OctylaminoCO. Fig. 3(a) shows that these two dyes have higher rates of fading in combination dyeings with Blue 165. Whatever values of $k_{0,i}$ they possess, compared with those for the above five dyes, the $k_{0,i}f_i$ values for these two dyes are the highest and next highest among the dyes used.

Since the $k_{0,i}$ values theoretically have a limit, their f_i values may increase (cf. Section 3.2, Table 5).

As mentioned in 3.1.2.3 (Table 2), Quinolone has many potential double bonds, while *n*-OctylaminoCO has a very limited number of double bonds. Applying Eq. (17) to the fading of these dyes in the combination dyeings with Blue 165 to determine their experimental $k_{0,i}/k_{0,\mathrm{B165}}$ values, the values give different explanations for the large rates of fading of these two dyes. This indicates the partial failure or incomplete realization of the analyses that led to Eqs. (14–17).

3.3.3. Effect of yellow filter on catalytic fading

In order to examine whether or not the high photosensitivity can be eliminated by yellow filtering, the exposure of the same dyeings to a carbon arc through a Y-51 yellow filter (which shields light of wavelengths < 510 nm) was carried out using four dyes. The exceptional fading behaviors of Quinolone and *n*-OctylaminoCO on PET were still observed, as shown in Fig. 3(b) and Table 5. The relative fading behaviors of the dyes of groups (2) and (3) were the same as those observed with direct exposure, although the rates of fading for the four dyes examined were decreased. Yellow 114 and Yellow 241 showed a small difference in their slopes of fading following exposure through the Y-51 yellow filter. This suggests that the two dyes possess high f_i values, which are not eliminated by the combination dyeings with Blue 165 or by exposure through the Y-51 yellow filter. The values of the slopes for the yellow dyes in the combination dyeings with Blue 165 are summarized in Table 5, as well as the decreases in the slops observed using the yellow filter. The rates of fading for the dyes of group (2) were reduced 15- to 30-fold compared with direct exposure, while those for the dyes of group (3) were reduced 10-fold. The photosensitization for group (2) was shielded differently by the filter compared to that for group (3). This suggests that the dyes of group (3) are photosensitized by longer wavelengths in the visible region, apart from the $\lambda_{\max}$. This indicates that the absorption of Blue 165 in the UV and visible regions at wavelengths >510 nm possesses the potential for photosensitization. Thus, all the dyes examined seem to have various effects on photosensitization by visible light. Apparently, the rates of fading in the combination dyeings depend not only upon the $k_{0,i}$ values, but also upon the f_i values.

3.3.4. Relative fading of yellow and Blue 165 in combination dyeings

In the 1:1 mixture dyeings where the f_i values are considerably low, sensitization may occur as follows:

$$[^3\mathrm{O}_2](f_{i\text{-Yellow}} + f_{\mathrm{Blue}})/2 < [^1\mathrm{O}_2] < [^3\mathrm{O}_2](f_{i\text{-Yellow}} + f_{\mathrm{Blue}}), \tag{18}$$

where $f_{i\text{-Yellow}}$ and f_{Blue} are the photosensitivity (−) for the *i*th yellow and blue disperse dye, respectively. The left-hand side of Inequality (18) describes the limit of non-dependence of concentration, and the right-hand side depicts the limit of complete dependence. Moreover, there must be an overlap of the absorption spectra for the two dyes on PET in the visible and UV regions. The effect of superposition may differ with the combination and the relative concentrations of the dyes. Although ideal experimental conditions to analyze catalytic fading have not been achieved, we carried out the present study as a preliminary experiment.

The term of photosensitization in Eq. (17) corresponding to both the sides of Inequality (18) is common to both the componential dyes or can be cancelled in the combination dyeings. If the reaction of the individual dyes with $^1\mathrm{O}_2$ in the combination dyeings occurs independently, the equation corresponding to Eq. (17) for the rates of fading for respective yellow dye and Blue 165 becomes:

$$\frac{\ln\frac{[D_{t,\mathrm{Yellow}}]}{[D_{0,\mathrm{Yellow}}]}}{\ln\frac{[D_{t,\mathrm{Blue165}}]}{[D_{0,\mathrm{Blue165}}]}} = -\left(\frac{k_{0,\mathrm{Yellow}}}{k_{0,\mathrm{Blue165}}}\right). \tag{19}$$

The rates of fading for Blue 165 in the combination dyeings were too small to estimate accurately the values of the parameters within a short exposure, except for combination dyeings with Quinolone and *n*-OctylaminoCO. Although the ratios of $k_{0,\mathrm{Yellow}}/k_{0,\mathrm{Blue165}}$ showed large scattering due to the short exposure, the ratios for long exposure could be determined. The results from direct exposure and from exposure through the Y-51 filter are listed in Tables 6 and 7, respectively.

The average experimental values of $k_{0,\mathrm{Yellow}}/k_{0,\mathrm{Blue165}}$ (by direct exposure) are listed, as well as the theoretical values from the MO calculation, in Table 6. Except for *n*-OctylaminoCO, the order of the experimental and theoretical values of $k_{0,\mathrm{Yellow}}/k_{0,\mathrm{Blue165}}$ almost coincide with each other, although the absolute values show some shifts. These situations are summarized in Table 1. This suggests that Eq. (19) describes rather well the values of $k_{0,\mathrm{Yellow}}/k_{0,\mathrm{Blue165}}$ in combination dyeings or in catalytic fading but that photosensitivity also influences the values. The discussion on photosensitivity for individual dyes is presented in Section 3.4. In the case of *n*-OctylaminoCO, the effect of photosensitivity described by the very high f_i value from the rate of fading of the single dyeings is apparent in the fading behaviors of the combination dyeings. The theoretical estimation of the $k_{0,i}$ values is regarded as showing unequivocally coincidence with the experimental values.

The experimental values of $k_{0,\mathrm{Yellow}}/k_{0,\mathrm{Blue165}}$ by exposure through the Y-51 filter are shown in Table 7. With the exception of *n*-OctylaminoCO, the orders of the ratios deduced by the two methods of exposure were almost identical, which indicates that the present simple analysis of catalytic fading on PET is applicable but insufficient. Moreover, the results indicate that the ratios of $k_{0,\mathrm{Yellow}}/k_{0,\mathrm{Blue165}}$ are strongly dependent upon the photosensitivity. This problem remains to be resolved.

Table 6
K/S values obtained from mixture dyeings with C.I. Disperse Blue 165 (629 nm) on exposure to a carbon arc in air

Dye (λ_{max} (nm))	Time of exposure (h)	Mixture dyeing					$k_{0,Yellow}/k_{0,B165}$		
		Yellow dye			Blue 165		Obsd.	Aver.	By MO (f_i)[b]
		K/S_{Orig}	K/S_{Red}	KSR[a]	K/S	KSR[a]			
Yellow 211 (451 nm)	0	8.450	8.006		10.160				
	5	8.122	7.678	0.959	10.138	0.998			
	10	8.040	7.607	0.950	9.900	0.974	1.94_7		
	20	7.927	7.495	0.936	9.875	0.972	2.32_8	2.30	4.8 (0.5)
	40	7.212	6.792	0.848	9.593	0.944	2.86_0		
	60	6.843	6.440	0.804	9.210	0.906	2.08_3		
Quinolone (437 nm)	0	9.032	8.568		9.989				
	5	7.781	7.329	0.855	9.738	0.975			
	10	7.245	6.797	0.793	9.653	0.966	6.70_5		
	20	5.663	5.224	0.610	9.454	0.946	8.90_5	8.34	7.2 (0.8)
	40	3.767	3.347	0.391	9.036	0.905	9.40_7		
	60	3.362	2.954	0.345	8.789	0.880	8.32_7		
n-OctylaminoCO (421 nm)	0	10.452	9.948		10.160				
	5	8.670	8.181	0.829	9.790	0.972			
	10	7.743	7.254	0.729	9.774	0.970	10.3_8		
	20	5.915	5.440	0.547	9.512	0.944	10.0_0	9.61	1.6 (9.9)
	40	2.978	2.541	0.255	8.746	0.868	9.65_0		
	60	2.680	2.258	0.227	8.437	0.838	8.39_2		
MeO2EtOCO (440 nm)	0	8.273	7.818		10.039				
	5	8.010	7.557	0.967	9.992	0.995			
	10	7.724	7.274	0.930	9.928	0.989	6.56_6		
	20	6.830	6.389	0.817	9.731	0.969	6.41_8	6.70	5.1 (0.6)
	40	5.555	5.123	0.655	9.525	0.949	8.08_3		
	60	5.232	4.814	0.616	9.227	0.919	5.73_5		
Yellow 114 (433 nm)	0	11.008	10.519		10.263				
	5	10.415	9.941	0.945	9.952	0.970			
	10	9.803	9.327	0.887	9.975	0.972	(4.22_2)		
	20	8.782	8.311	0.790	9.875	0.962	6.08_4	7.05	6.2 (0.4)
	40	7.162	6.697	0.637	9.626	0.938	8.97_6		
	60	6.750	6.291	0.598	9.616	0.937	8.03_2		
Yellow 241 (438 nm)	0	9.542	9.075		10.179				
	5	9.106	8.651	0.953	9.914	0.974			
	10	8.881	8.425	0.928	9.942	0.977	(3.21_1)		
	20	7.880	7.434	0.819	9.720	0.955	4.33_6	5.12	3.3 (1.0)
	40	6.467	6.026	0.664	9.608	0.944	7.10_5		
	60	5.974	5.553	0.612	9.164	0.919	5.81_2		
NitropentanoxyCO (449 nm)	0	8.442	8.004		9.978				
	5	8.275	7.838	0.979	9.956	0.998			
	10	8.189	7.754	0.969	9.898	0.991	(3.48_3)		
	20	7.673	7.250	0.906	9.631	0.965	2.77_0	2.78	4.8 (0.4)
	40	7.245	6.832	0.854	9.406	0.943	2.68_9		
	60	7.153	6.740	0.842	9.410	0.943	2.87_8		
Single dyeing									
Blue 165 (629 nm)	0				10.396				
	5				10.463	1.0			
	10				9.450	0.909			
	20				9.582	0.922			
	40				9.427	0.909			
	60				9.359	0.900			

[a] K/S ratio = KSR = $(K/S)_t/(K/S)_0$.
[b] $k_{0,Yellow}/k_{0,B165}$ by MO method (f_i/f_{B165}) (cf. Table 5).

3.4. LF of pyridone-azo dyes and their potential properties

PET absorbs considerable amounts of oxygen, which results in the photo-oxidative fading of disperse dyes on exposed PET fabrics. As the first approximation, the fading can be attributed to the reaction of dyes with $^1O_2$, which is generated by the self-photosensitization of the dyes, as in the case of reactive dyes on cellulose [3–5]. Thus, the rates or slopes of photo-fading are proportional to the product of

Table 7
K/S values obtained from mixture dyeings with C.I. Disperse Blue 165 (629 nm) exposed to a carbon arc through Y-51 filter

Dye (λ_{max} (nm))	Time of exposure (h)	Mixture dyeing					$k_{0,Yellow}/k_{0,Blue}$		
		Yellow dye			Blue 165		Obs.	Aver.	By MO (f_i)[b]
		K/S_{Orig}	K/S_{Red}	KSR[a]	K/S	KSR[a]			
Quinolone (437 nm)	0	9.032	8.568		9.989				
	40	8.272	7.803	0.911	10.097	0.99			
	80	7.554	7.106	0.829	9.639	0.965	5.26	4.6	7.2 (0.8)
	120	6.943	6.511	0.760	9.307	0.932	3.90		
n-OctylaminoCO (421 nm)	0	10.452	9.948		10.073				
	40	9.122	8.515	0.856	9.875	0.981			
	80	8.212	7.801	0.784	9.756	0.969	5.47	5.7	1.6 (9.9)
	120	7.199	6.728	0.676	9.416	0.935	5.83		
Yellow 114 (433 nm)	0	11.008	10.519		10.263				
	40	10.545	10.057	0.956	10.240	0.998			
	80	10.462	9.983	0.949	10.055	0.980	2.27	2.2	6.2 (0.4)
	120	10.358	9.882	0.939	9.980	0.972	2.22		
Yellow 241 (438 nm)	0	9.542	9.082		10.018				
	40	9.450	8.990	0.990	10.026	0.995			
	80	9.336	8.881	0.978	9.919	0.990	2.21	2.0	3.3 (1.0)
	120	9.190	8.740	0.962	9.810	0.979	1.83		

[a] K/S ratio = KSR = $(K/S)_t/(K/S)_0$.
[b] $k_{0,Yellow}/k_{0,B165}$ by MO method (f_i/f_{B165}) (cf. Table 5).

$k_{0,i}$ and f_i, as well as to the LF ratings, as summarized in Table 1.

From the rates of fading of single dyeings of PET substrate, the order of the LF for the yellow dyes examined is as follows:

$$\text{NitropentanoxyCO} \geq \text{Yellow 211} > \text{Yellow 114} > \text{MeO2EtOCO} > \text{Yellow 241} > \text{Quinolone} \gg n\text{-OctylaminoCO}. \quad (20)$$

Disperse pyridone-azo and quinolone-azo dyes possess a wide range of f_i values.

(1) C.I. Disperse Yellow 211 and NitropentanoxyCO: According to frontier orbital theory [22–25], Yellow 211 possesses a lower value of $S_{m,n}^{(E)}$ towards $^1O_2$ (cf. Section 3.1), being the lowest value next to Blue 165 and *n*-OctylaminoCO, than that for NitropentanoxyCO. The latter dye has the lowest value of f_i among the dyes examined, and has a value of $k_{0,i}$ that is similar to those of the dyes of group (2). Since they possess, as a whole, low values of f_i, they have excellent LF, which is attributed to the relatively low values of $k_{0,i}$ and f_i.
(2) Yellow 241, Yellow 114 and MeO2EtOCO: The $S_{m,n}^{(E)}$ values estimated by the MO method for the three dyes were regarded as being almost identical, which was confirmed by experiments using the combination dyeings with Blue 165. Their reactivities towards $^1O_2$ were estimated to be 1.5-fold higher than those for the dyes of group (1). Thus, Yellow 241 has an LF rating of 5, which is a little lower than those of the other two dyes, and is estimated to possess a slightly higher value of f_i. In order to endow dyes with excellent LF, the dyes must have low values of k_0 as well as low values of f_i.
(3) *n*-OctylaminoCO: Although this dye possesses lower $S_{m,n}^{(E)}$ values than those for the dyes of groups (1) and (2), it exhibits the lowest LF among the dyes examined, due to having the largest f_i value. We could not find the reason why this dye has structurally the highest value of f_i among the dyes examined.
(4) Quinolone: Although this dye comprises a heterocycle and is different from the other dyes, the $S_{m,n}^{(E)}$ value was higher than those for the dyes of groups (1) and (2), as estimated using the PM5 method. However, analyses of catalytic fading as well as the fading of single dyeings indicate that the present MO treatment is reasonable, resulting in a reasonable interpretation based on the present model for the photo-fading of disperse dyes on PET substrates, as summarized in Tables 1 and 5. Whether or not this conclusion is completely accurate must be confirmed by estimating the photochemical properties of this dye using another method.

3.5. LF on the PET substrate

The photo-fading of disperse dyes on the PET substrate upon exposure in air is essentially oxidative and similar

to the fading on a cellulose substrate. From the viewpoint of the present model, both the $k_{0,i}$ and f_i values contribute with the same weight to the rates of photo-oxidative fading. In practice, however, the range of their values was considerably different. The values of $k_{0,i}$ and f_i for disperse dyes lie in a rather narrow range of order, although those of f_i for reactive dyes range over several orders [28]. This is because it is not possible to make the electrophilic frontier density negligibly small, while many factors contribute to photosensitivity.

Thus, the following conclusions can be drawn from the present study:

1. The lower the f_i values, the higher the LF.
2. A dye with a low f_i value possesses a moderate LF rating, even if the dye has a high $k_{0,i}$ value.
3. The performance of a dye with a large f_i value is strongly influenced by the $k_{0,i}$ values; the dye exerts a harmful effect on the partner dyes as well as on itself, especially when it has a high $k_{0,i}$ value, catalytic fading of the partner dye and low LF.
4. The apparent photosensitivity of mixture dyeings of PET is lower than simple additivity, and is sensitive to the combination of dyes due to the superposition of absorption spectra.

Table 8
Photo-fading of seven yellow dyes dyed in admixture with Blue 165 and Blue 56 and of their single dyeings of PET fabrics on exposure to a carbon arc in air

No.	Dye	Depth	Time (h)	CIE parameters measured						
				X	*Y*	*Z*	ΔE^*_{ab}	ΔL^*	Δa^*	Δb^*
Fading of single dyeings										
1	Yellow 211	*N*/2	0	65.64	70.76	9.09				
			40	64.48	69.30	10.04	4.26	−0.72	0.47	−4.18
2	Quinolone	*N*/2	0	64.27	69.75	10.52				
			40	63.51	68.42	13.81	9.96	−0.65	1.10	−9.89
3	*n*-OctylaminoCO	*N*/2	0	65.72	73.72	13.38				
			40	65.41	72.19	19.14	14.16	−0.73	2.45	−13.92
4	MeO2EtOCO	*N*/2	0	66.14	74.14	10.58				
			40	65.77	73.59	12.10	4.69	−0.26	0.30	−4.67
5	Yellow 114	*N*/2	0	66.26	75.86	11.34				
			40	64.01	73.04	12.39	5.34	−1.32	0.09	−5.12
6	Yellow 241	*N*/2	0	66.22	73.94	9.99				
			40	65.15	72.88	11.92	6.39	−0.51	−0.24	−6.39
7	Nitropentanoxy	*N*/2	0	65.78	74.47	11.09				
			40	65.40	73.38	11.87	3.37	−0.51	1.36	−3.02
8	Blue 165	*N*/3	0	13.54	15.57	40.41				
			40	13.94	16.05	40.30	1.39	0.63	−0.17	1.22
9	Blue 56	*N*/3	0	14.76	15.46	43.09				
			20	14.61	15.28	42.17	0.69	−0.24	0.12	0.64
			40	14.45	15.15	41.37	1.35	−0.42	−0.06	1.27
			60	14.71	15.49	41.22	2.28	0.04	−0.44	2.23
Fading of mixture dyeings with C.I. Disperse Blue 165 (N/3)										
1	Yellow 211	*N*/2	0	7.82	12.19	7.52				
			40	8.14	12.38	8.40	3.06	0.30	1.68	−2.60
2	Quinolone	*N*/2	0	8.08	13.16	8.44				
			40	9.34	13.90	14.10	15.44	1.09	6.18	−14.10
3	*n*-OctylaminoCO	*N*/2	0	8.02	13.39	10.11				
			40	9.98	14.21	18.15	21.03	1.19	11.48	−17.55
4	MeO2EtOCO	*N*/2	0	8.01	13.13	8.52				
			40	8.58	13.42	10.93	7.41	1.45	3.16	−6.67
5	Yellow 114	*N*/2	0	7.74	13.22	8.15				
			40	8.41	13.68	10.43	6.87	0.68	3.12	−6.09
6	Yellow 241	*N*/2	0	7.85	12.88	7.71				
			40	8.38	13.27	9.95	6.77	0.58	2.31	−6.38
7	Nitropentanoxy	*N*/2	0	7.99	13.27	8.52				
			40	8.37	13.49	9.29	2.79	0.34	1.93	−1.96
Fading of mixture dyeings with C.I. Disperse Blue 56 (N/3)										
1	Yellow 211	*N*/2	0	8.39	12.03	7.76				
			40	8.67	12.18	8.63	2.98	0.23	1.38	−2.58
2	Quinolone	*N*/2	0	8.45	12.70	8.46				
			40	9.02	12.93	11.15	8.39	0.35	3.40	7.66
3	*n*-OctylaminoCO	*N*/2	0	8.38	12.89	10.19				
			40	9.32	13.32	13.95	10.41	0.65	5.19	−8.95

3.6. Assessment of catalytic fading

Although the present analyses of catalytic fading are still not comprehensive, many observed features are extracted and some problems remain to be resolved. Unfortunately, we could find neither a strong all-around photo-sensitizer (such as Rose Bengal) nor an appropriate diagnostic agent with a high $k_{0,i}$ value and low f_i value (such as Pyr-Yellow) to examine photosensitivity [18].

From the results of the present study, the only method that was able to examine the mutual fading behavior of componential dyes on PET fabrics was the procedure using the Kubelka–Munk parameter from the reflectance curve, although the combination of yellow and blue dyes for green dyeings may bring about the largest separation in the λ_{max} between the componential dyes. In this section, comparing the results of the analyses in the former sections with the values of the chromaticity parameters of the exposed fabrics, the utility of the CIELAB method is discussed.

3.6.1. Features of catalytic fading

To simplify the problems, the catalytic fading of a two component mixture is discussed.

1. Combination dyeings from two components whose values of $k_{0,i}$ are different from each other regardless of the f_i values generally suffer from off-tone fading. The on-tone fading of combination dyeings occurs very rarely.
2. From the results of present study, dyes with higher $k_{0,i}$ values suffer fading more easily, while dyes with higher f_i values promote catalytic fading.
3. The fading is called catalytic fading when the rates of fading for either or both components of the combination dyeings, the concentrations of which are equal, are accelerated compared with the rates of fading for each component in the single dyeings. Since the PET fabric-disperse dye system is heterogeneous, the rates of fading show strong concentration dependence. If the restriction of same concentration is eliminated, one can find many dyes that cause or suffer catalytic fading.
4. In the present study, the 1:1 combination dyeings, the concentrations of which were the same in the single and combination dyeings, were used to eliminate the effects of concentration dependence on the catalytic fading. However, the total concentration is doubled and the increase in the total concentration must have some effects. The overlapping of the absorption spectra is inevitable. The photosensitivity of the mixture must be lower than the sum of f_i, and a scavenging effect due to the total increase in the concentration must exist. Thus, the prerequisite of catalytic fading may fulfill no simple additivity and many interaction factors may act to lower the additivity. Since the reduced additivity becomes larger than the f_i value of the componential dye, the combination of dyes with high f_i values may cause catalytic fading.

3.6.2. Chromaticity parameters of dyes after exposure

The results of the measurements of the exposed PET fabrics dyed singly and in admixture with Blue 165 and seven yellow dyes are listed in Table 8, and the corresponding Kubelka–Munk parameters for the mixture dyeings are listed in Table 6. The results for Blue 56 are shown in Table 8 and their Kubelka–Munk parameters are shown in Table 9. In these tables, the data for the original sample and samples exposed for 40 h are listed.

Combination with Blue 165: Among the combination dyeings of yellow and blue dyes, the rates of fading for the two yellow dyes, Yellow 211 and Nitropentanoxy, were decreased by the combination with Blue 165, while the rates for the other

Table 9
K/S values obtained from mixture dyeings with C.I. Disperse Blue 56 (636 nm)

Dye (λ_{max} (nm))	Time of exposure (h)	Mixture dyeing					Single dyeing Yellow	
		Yellow dye			Blue 56			
		K/S_{Orig}	K/S_{Red}	KSR[a]	K/S	KSR[a]	K/S	KSR[a]
Yellow 211 (451 nm)	0	8.057	7.628		6.433		7.975	
	20	7.368	6.929	0.908	6.136	0.954	7.246	0.909
	40	6.955	6.489	0.851	6.210	0.965	6.842	0.858
Quinolone (437 nm)	0	8.486	8.132		6.368		8.193	
	20	6.408	6.033	0.742	6.303	0.990	6.050	0.738
	40	5.413	5.021	0.617	6.121	0.961	4.942	0.603
n-OctylaminoCO (421 nm)	0	10.267	9.961		6.688		10.061	
	20	6.339	6.026	0.605	6.400	0.957	6.797	0.676
	40	6.074	4.749	0.477	6.209	0.928	4.118	0.409
Single dyeing Blue 56 (636 nm)	0				6.360			
	20				6.262	0.984		
	40				6.234	0.980		
	60				5.879	0.924		

[a] K/S ratio = KSR = $(K/S)_t/(K/S)_0$.

five yellow dyes were increased, compared with the rates for the single dyeings at the corresponding concentrations. Even if these results are known from Table 5, in which the *K*/*S* parameters were used, it is not possible to deduce these results from Table 8. The chromaticity parameters of the combination dyeings are not useful in analyzing the fading of the two components.

Combination with Blue 56: In order to compare the influences of the blue dyes in catalytic fading, the fading of combination dyeings with Blue 56, which is known as a typical non-eating blue dye, with three yellow dyes was examined. Inspecting the data listed in Tables 8 and 9, the rates of fading for the combination dyeings are promoted a little for Yellow 211 and considerably for Blue 56, compared with those for the single dyeings, as indicated in Table 9. It was confirmed that *n*-OctylaminoCO had little negative influence on the fading of Blue 56. Although the extent of negative influence is small, Blue 56 is not always a safe blue dye component for green dyeings. These results can be derived only from the *K*/*S* parameters (Table 9) and not from the CIE parameters (Table 8).

The reasons why these dyes exhibit such fading behaviors in the combination dyeings of PET and the detailed molecular mechanism of photosensitization, remain to be elucidated.

4. Summary

Photo-fading of disperse azo dyes derived from pyridone (six) and quinolone (one) rings in the single and combination dyeings of PET was analyzed to elucidate the mechanism of fading upon exposure in air. Catalytic fading of the dyes by a yellow-eating dye, C.I. Disperse Blue 165, was also analyzed.

Almost all the yellow dyes, with the exception of C.I. Disperse Yellow 211 and NitropentanoxyCO, had promoting effects on the rate of fading for the blue dye in the 1:1 combination dyeings of PET fabric, compared with the rates for the single dyeings. The fading of azo dyes in the single and combination dyeings of PET can be explained by the photo-oxidation of the dyes (the second-order rate constant: k_0), with $^1O_2$ generated by the sensitization of the dyes (the quantum yield: f) as the photo-sensitizer.

It was confirmed that the rates of fading in the single dyeings are proportional to the product of k_0 and f. The k_0 values for yellow azo dyes are consistent with the estimation deduced from the sum of the electrophilic frontier electron densities of the potential double bonds in the dye molecule, as calculated by the PM5 method.

The substituents of the diazo components of the pyridone-azo dyes had some influence on the distribution d_{HOMO} in the diazo component but had little influence on the distribution d_{HOMO} in the pyridone ring. The nitro groups in the two dyes decreased to the limit of reactivity the d_{HOMO} in the diazo component.

C.I. Disperse Blue 56 is not always a safe blue dye component for green dyeings. The analysis of fading for componential dyes in combination dyeings is possible using Kubelka–Munk (*K*/*S*) parameters but not using CIE chromaticity parameters.

Acknowledgement

This work was supported by a Grant-in-Aid for Scientific Research from the Ministry of Education, Culture, Sports, Science and Technology, Japan.

References

[1] Rouette H-K. Encyclopedia of textile finishing. Berlin: Springer; 2001.
[2] Okada Y, Hirose M, Kato T, Motomura H, Morita Z. Photofading of vinylsulfonyl reactive dyes on cellulose under wet conditions. Dyes and Pigments 1990;14(2):113–27.
[3] Okada Y, Hirose M, Kato T, Motomura H, Morita Z. Fading of vinylsulfonyl reactive dyes on cellulose in admixture under wet conditions. Dyes and Pigments 1990;14(4):265–85.
[4] Okada Y, Motomura H, Morita Z. Photosensitization and simultaneous reductive or oxidative fading of monochlorotriazinyl reactive dyes on cellulose under wet conditions. Dyes and Pigments 1992;20(2):123–35.
[5] Hihara T, Okada Y, Morita Z. Photo-oxidation and -reduction of vat dyes on water-swollen cellulose and their lightfastness on dry cellulose. Dyes and Pigments 2002;53(2):153–77.
[6] Hihara T, Okada Y, Morita Z. Photo-oxidation of pyrazolinylazo dyes and analysis of reactivity as azo and hydrazone tautomers using semiempirical molecular orbital PM5 method. Dyes and Pigments 2006;69(2):151–76.
[7] Hihara T, Okada Y, Morita Z. Photo-oxidation of reactive azobenzene dyes and an analysis of their reactivity for the azo and hydrazone tautomers using semiempirical molecular orbital PM5 method. Dyes and Pigments 2007;75(1):225–45.
[8] Hihara T, Okada Y, Morita Z. A semiempirical molecular orbital study on the photo-reactivity of monoazo reactive dyes derived from γ- and J-acid. Dyes and Pigments 2007;73(2):141–61.
[9] Hihara T, Okada Y, Morita Z. An analysis of the photo-reactivity of monoazo reactive dyes derived from H-acid and related naphthalene sulfonic acids using the PM5 method. Dyes and Pigments 2007;75(3):585–605.
[10] Giles CH, Forrester SD. Physical factors affecting the light stability of dyed and pigmented polymers. In: Allen NS, McKellar JF, editors. Photochemistry of dyed and pigmented polymers. Essex: Applied Science Publishers Ltd; 1980. p. 51–91 [chapter 2].
[11] Evans NA. Structural factors affecting light stability of dyed polymers. In: Allen NS, McKellar JF, editors. Photochemistry of dyed and pigmented polymers. Essex: Applied Science Publishers Ltd; 1980. p. 93–159 [chapter 3].
[12] Rembold MW, Kramer HEA. Singlet oxygen as an intermediate in the catalytic fading of dye mixtures. The Journal of the Society of Dyers and Colourists 1978;94(1):12–7.
[13] Griffiths J, Hawkins C. Mechanistic aspects of the photochemistry of dyes and their intermediates, II – Evidence for the formation of singlet oxygen by phototendering vat dyes. The Journal of the Society of Dyers and Colourists 1973;89(2):173–7.
[14] Griffiths J. Solution and polymer photochemistry of azo dyes and related compounds. In: Allen NS, editor. Developments in polymer photochemistry, vol. 1. Essex: Applied Science Publishers Ltd; 1980. p. 145–90 [chapter 6].
[15] Okada Y, Kato T, Motomura H, Morita Z. Catalytic fading of vinylsulfonyl reactive dye mixtures on cellulose under wet conditions. Dyes and Pigments 1990;12(3):197–211.
[16] Duff DG, Sinclair RS. Giles's laboratory course in dyeing. fourth ed.). Bradford: The Society of Dyers and Colourists; 1989.
[17] CAChe Reference Guide [CAChe Reference Guide 4.9; 3-9–3-10], Fujitsu Ltd; 2002.
[18] Hihara T, Okada Y, Morita Z. Azo–hydrazone tautomerism of phenylazonaphthol sulfonates and their analysis using the semiempirical molecular orbital PM5 method. Dyes and Pigments 2003;59(1):25–41.
[19] Hihara T, Okada Y, Morita Z. Reactivity of phenylazonaphthol sulfonates, their estimation by semiempirical molecular orbital PM5 method,

and the relation between their reactivity and azo–hydrazone tautomerism. Dyes and Pigments 2003;59(3):201–22.
[20] Iesce MR, Cermola F, Temussi F. Photooxygenation of heterocycles. Current Organic Chemistry 2005;9(2):109–39.
[21] Fukui K, Fujimoto H, editors. Frontier orbitals and reaction paths: selected papers of Fukui K. World Scientific series in 20th century chemistry, vol. 7. Singapore: World Scientific; 1997.
[22] Fukui K, Yonezawa T, Shingu H. A molecular orbital theory of reactivity in aromatic hydrocarbons. Journal of Chemical Physics 1952;20(4):722–5.
[23] Fukui K, Yonezawa T, Nagata C, Shingu H. Molecular orbital theory of orientation in aromatic, heteroaromatic and other conjugated molecules. Journal of Chemical Physics 1954;22(8):1433–42.
[24] Fukui K, Yonezawa T, Nagata C. Interrelations of quantum-mechanical quantities concerning chemical reactivity of conjugated molecules. Journal of Chemical Physics 1957;26(4):831–41.
[25] Matsumoto M, Yamada M, Watanabe N. Reversible 1,4-cycloaddition of singlet oxygen to *N*-substituted 2-pyridones: 1,4-endoperoxide as a versatile chemical source of singlet oxygen. Chemical Communications 2005;4:483–5.
[26] Rabek JF. 1.3 Absorption of radiation, Mechanisms of photophysical processes and photochemical reactions in polymers. New York: Wiley; 1987. p. 5–9.
[27] Vieth WR, Alcalay HH, Frabetti AJ. Solution of gases in oriented poly-(ethylene terephthalate). Journal of Applied Polymer Science 1964;8(5): 2125–38.
[28] Hihara T, Okada Y, Morita Z. Relationship between photochemical properties and colourfastness due to light-related effects on monoazo reactive dyes derived from H-acid, γ-acid, and related naphthalene sulfonic acids. Dyes and Pigments 2004;60(1): 23–48.